

the tunnel current while slowly varying the time delay between pump and probe.

As with many experiments using near-field probes, the key to success lies in suppressing spurious effects while boosting the desired signal above the noise floor. Shigekawa and colleagues demonstrate a clever lock-in detection scheme akin to heterodyne detection in a radio receiver to boost their sensitivity and isolate the spin-dependent signal while keeping the average laser power impinging on the tip constant. Maintaining a constant power that is absorbed by the tip is an essential step to avoid spurious signals related to time-dependent heating, which have plagued laser-combined STM in the past⁷.

An important aspect of the experiment is the non-local nature of the optical excitation. The micrometre-sized laser beam presents a global excitation compared with the tunnel current detection, which is localized on the ångström scale. It is possible that many photoexcited electrons, not just those generated immediately under the scanning tunnelling microscope tip, are detected at each pump–probe cycle. Consequently, this measurement scheme may also be applicable to the study of non-local effects, such as spin diffusion in real space. It also opens the door to take other established methods in ultrafast optics to the nanoscale, such as the resonant excitation of phonons⁸. Reliance on a global excitation, however, also creates a challenge for other sample systems, such as metals, where vanishing optical penetration depth

significantly reduces the excitation volume and may preclude the application of laser-combined STM. Surmounting this challenge will be important for expanding the scope of this technique. Local enhancement of the light intensity under the tip, as achieved, for example, with plasmonic waveguides⁹, could overcome limitations in excitation efficiency and reach the same highly localized control as approaches employing fast gating of the tunnel junction voltage^{5,6}.

Perhaps the most important finding of the work by Shigekawa and colleagues is the measurement of spin dynamics beyond population decay, showing that the scanning tunnelling microscope can detect coherent spin precession with high fidelity. Hallmark features are the detection of the quantum beat of the spin polarization in a magnetic field¹⁰ and its resonant amplification with matched laser-pulse repetition¹¹.

Electron spins in semiconductors can maintain quantum–mechanical coherence only for short periods of time. In this time, they can, in principle, be used for spintronic applications that go further than static magnetoresistance. The method demonstrated by Shigekawa and colleagues is the first that is sensitive to spin coherence at nanometre length-scales. Decoherence and relaxation of spins in semiconductors is governed by nanometre-sized interactions with defects and disorder potentials. Understanding these processes is of key importance in the engineering of devices that harness spin coherence exceeding nanoseconds. With the local detection

mechanism established, many questions could now be answered. For example, how spatially uniform is the spin coherence? What role do defects play in the emission of spin waves? What is the influence of interface disorder on spin injection across device layers?

Spatial heterogeneity in solids is intricately linked to the observable dynamics therein. Combining STM with pump–probe measurement schemes, as exemplified by the work of Shigekawa and colleagues, presents a new generation of scanning probe experiments that access elementary processes at their intrinsic length- and timescales. □

Sebastian Loth, Jacob A. J. Burgess and Shichao Yan are at the Max Planck Institute for the Structure and Dynamics of Matter, 22761 Hamburg, Germany, and the Max Planck Institute for Solid State Research, 70569 Stuttgart, Germany. e-mail: sebastian.loth@mps.d.mpg.de

References

1. Sih, V. *et al. Nature Phys.* **1**, 31–35 (2005).
2. Bolte, M. *et al. Phys. Rev. Lett.* **100**, 176601 (2008).
3. Yoshida, S. *et al. Nature Nanotech.* **9**, 588–593 (2014).
4. Terada, Y., Yoshida, S., Takeuchi, O. & Shigekawa, H. *Nature Photon.* **4**, 869–874 (2010).
5. Cocker, T. L. *et al. Nature Photon.* **7**, 620–625 (2013).
6. Loth, S., Eitzkorn, M., Lutz, C. P., Eigler, D. M. & Heinrich, A. J. *Science* **329**, 1628–1630 (2010).
7. Gerstner, V., Knoll, A., Pfeiffer, W., Thon, A. & Gerber, G. *J. Appl. Phys.* **88**, 4851–4859 (2000).
8. Först, M. *et al. Nature Phys.* **7**, 854–856 (2011).
9. Neacsu, C. C. *et al. Nano Lett.* **10**, 592–596 (2010).
10. Bar-Ad, S. & Bar-Joseph, I. *Phys. Rev. Lett.* **66**, 2491–2494 (1991).
11. Kikkawa, J. M. & Awschalom, D. D. *Phys. Rev. Lett.* **80**, 4313–4316 (1998).

GRAPHENE

Electrons en masse

Massless electrons in graphene exhibit a mass when considered as collective excitations known as plasmons.

Fengnian Xia

A plasmon is the quantum of collective motion of charged carriers and typical plasmonic materials are noble metals such as silver and gold, which have many free electrons^{1,2}. Plasmons have attracted significant interest recently due to their ability to confine light below the diffraction limit. In dielectric materials, light diffraction is a result of the uncertainty principle: limitations to the value of the refractive index of the material, n , cause restrictions in momentum, k , space ($k = n\omega/c$, where ω is the angular frequency of the light and c is the speed of the light

in vacuum), resulting in a spreading of the light in real space. Plasmon waves in metallic waveguides³ or at metal/dielectric interfaces can overcome this fundamental limit by leveraging the negative permittivity of metals, which arises from the collective inertia of electrons under time-varying electric fields, and is usually in the near-infrared to visible frequency range. From the perspective of circuit analysis, this negative but real permittivity corresponds to an imaginary conductivity, revealing the inductive character of the metal. Such an inductance is called ‘kinetic inductance’, to

differentiate it from the traditional ‘magnetic inductance’, which results from a magnetic field around a current-carrying conductor. For normal metals, the kinetic inductance can be safely ignored at microwave frequencies because their resistance dominates the impedance at this relatively low-frequency range. In superconductors, the kinetic inductance can be significant even at microwave frequencies due to their ideal conductive properties⁴.

Writing in *Nature Nanotechnology*, Donhee Ham, Philip Kim and colleagues at Harvard University, Columbia University

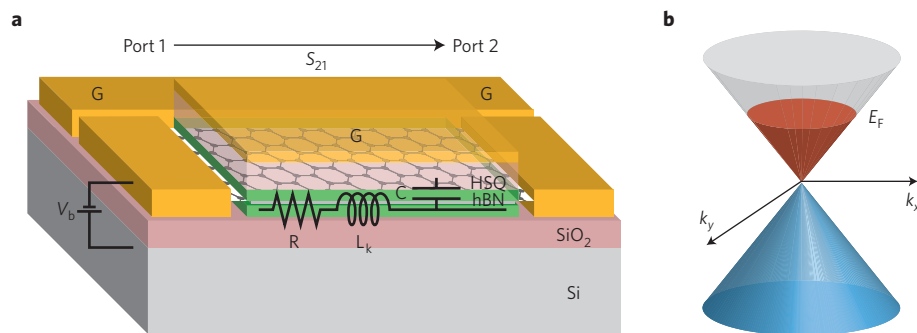


Figure 1 | Graphene kinetic inductance. **a**, Schematic of the graphene device used for microwave measurements. The graphene is sandwiched between two hexagonal boron nitride (hBN) layers (green). The top-gate dielectric consists of an hBN layer and a thin layer of hydrogen silsesquioxane (HSQ) on top of the hBN. A radiofrequency signal is sent from port 1 and the transmission signal is measured from port 2; from this, the kinetic inductance is inferred. S_{21} is the complex transmission coefficient, which refers to the transmitted signal at port 2 over the input signal at port 1. Here G and S denote ground and signal pads, respectively. The equivalent circuit shows the resistor R , whose resistance models the carrier scattering in graphene, the kinetic inductor, L_k , and the gate capacitor, C . A bias voltage V_b is used to tune the plasmon mass. **b**, The energy dispersion in graphene around the K point, $E = \hbar k v_f$, where \hbar is the reduced Planck constant, k is the wavevector measured from the K point and v_f is the Fermi velocity. Owing to the relativistic nature of the energy dispersion, the carrier mass at the Fermi level is $m = E_f/v_f^2 = \hbar k_f/v_f$, where k_f is the Fermi vector. Electron levels (red) are filled up to the Fermi level. All the hole states (blue) are occupied.

and National Institute for Materials Science in Tsukuba have now explored kinetic inductance in graphene through delicate microwave phase-delay measurements (Fig. 1a)⁵. These measurements are challenging because the phase information is buried under electron scattering, which causes a resistance, represented by the resistor, R , in the equivalent circuit in Fig. 1a. The researchers addressed this problem by sandwiching the graphene between two layers of hexagonal boron nitride, another two-dimensional material that can be used as a dielectric for the gating of graphene⁶. This arrangement prevents the carriers in graphene from being scattered by external sources, leading to a carrier mobility as high as $390,000 \text{ cm}^2 \text{ V}^{-1} \text{ s}^{-1}$ at 30 K. Furthermore, the proximate gate capacitor, C , that is created by using the hexagonal boron nitride and hydrogen silsesquioxane as a dielectric enhances the phase delay, making it much larger than the intrinsic phase noise of the measurement set-up. These two innovations allow the phase delay induced by the kinetic inductance to be accurately measured, and from this the plasmonic properties of graphene can be inferred.

The researchers tune the doping of graphene by applying a bias voltage V_b to the proximate gate, and show that the ‘plasmon

mass’ in graphene depends on the Fermi level. Such a Fermi-energy-dependence of the plasmon mass is due to the linear energy dispersion of Dirac relativistic electrons, which resembles that of photons (with the velocity of the light in vacuum c replaced by the Fermi velocity v_f ; Fig. 1b). The collective motion of carriers in real space can be interpreted as the oscillation of the Fermi surface in momentum space, with only the carriers close to it deviating from their equilibrium states⁵. At the Fermi surface, the Fermi energy is $E_f = m v_f^2$, according to Einstein’s energy–mass relation, where m is the electron mass. As a result, discrete relativistic band electrons with zero rest mass show a collective mass determined by the Fermi level. Although such a Fermi-energy-dependent mass in graphene has already been explored theoretically and confirmed experimentally^{7–12}, the work of Ham and colleagues is a direct measurement of the phase delay due to collective carrier inertia, from which the plasmon mass is immediately inferred.

Besides its scientific significance, the work of Ham and colleagues may also have implications for radiofrequency electronics. The graphene kinetic inductance is much larger than the traditional magnetic inductance, and magnetic inductors normally occupy large areas on the

microwave chip. Therefore, replacing magnetic inductors with kinetic ones made of graphene may lead to the overall miniaturization of circuits. Furthermore, an inductor that makes use of the kinetic inductance can be tuned by changing the carrier concentration in the graphene layer using an external voltage, leading to voltage-controlled solid-state inductors, which can be integrated with other electronic components.

The potential applications of graphene plasmons also go beyond radiofrequency electronics. Plasmons in semi-metallic graphene can occupy a spectral range from microwave to mid-infrared, and the tunable carrier density in graphene adds another important degree of freedom, which is not available in metals. Moreover, the plasmon damping in graphene might be significantly suppressed through the optimization of graphene growth, leading to longer propagation length of the plasmon–polariton wave. Recently, various approaches have been utilized to explore plasmons in graphene. For example, it has been shown that plasmon–polaritons in graphene can be excited using a specially configured scanning near-field optical microscope (SNOM), with the momentum of the plasmon–polariton wave provided by the spatially confined SNOM tip^{13,14}. Various graphene micro- and nanostructures have also been demonstrated to support localized plasmons^{11,12}. Further improvements in the design and properties of these graphene plasmonic devices could lead to a range of scientific discoveries and applications in areas such as radiofrequency electronics, mid-infrared light detection and modulation, chemical sensing, and thermal imaging. □

Fengnian Xia is in the Department of Electrical Engineering, Yale University, 15 Prospect Street, New Haven, Connecticut 06511, USA.
e-mail: fengnian.xia@yale.edu

References

- Maier, S. *et al.* *Adv. Mater.* **13**, 1501–1505 (2001).
- Brongersma, M. & Shalae, V. *Science* **328**, 440–441 (2010).
- Takahara, J., Yamagishi, S., Taki, H., Morimoto, A. & Kobayashi, T. *Opt. Lett.* **22**, 475–477 (1997).
- Annunziata, A. *et al.* *Nanotechnology* **21**, 445202 (2010).
- Yoon, H. *et al.* *Nature Nanotech.* **9**, 594–599 (2014).
- Dean, C. *et al.* *Nature Nanotech.* **5**, 722–726 (2010).
- Novoselov, K. S. *et al.* *Nature* **438**, 197–200 (2005).
- Wunsch, B., Stauber, T. & Guinea, F. *New J. Phys.* **8**, 318 (2006).
- Hwang, E. H. & Das Sarma, S. *Phys. Rev. B* **75**, 205418 (2007).
- Abedinpour, S. *et al.* *Phys. Rev. B* **84**, 045429 (2011).
- Ju, L. *et al.* *Nature Nanotech.* **6**, 630–634 (2011).
- Yan, H. *et al.* *Nature Nanotech.* **7**, 330–334 (2012).
- Fei, Z. *et al.* *Nature* **487**, 82–85 (2012).
- Chen, J. *et al.* *Nature* **487**, 77–81 (2012).